Geoelectrical Inference of Mass-Transfer Parameters Using Temporal Moments

by Frederick D. Day-Lewis[1] and Kamini Singha[2]

[1]U.S. Geological Survey, Office of Ground Water, Branch of Geophysics, 11 Sherman Place, Unit 5015, Storrs CT 06269

[2]The Pennsylvania State University, 311 Deike Building, University Park PA 16802

Corresponding Author:

Fred Day-Lewis

Email: daylewis@usgs.gov

Phone: 860.487.7402 x21; Fax: 860.487.8802

Final copy as submitted to Water Resources Research for publication as: Day-Lewis F.D. and Singha, K., 2008, Geoelectrical inference of mass transfer parameters using temporal moments: Water Resour. Res., 44, W05201, doi:10.1029/2007WR006750.

Abstract

We present an approach to infer mass-transfer parameters based on (1) an analytical model that relates the temporal moments of mobile and bulk concentration; and (2) a bicontinuum modification to Archie's Law. Whereas conventional geochemical measurements preferentially sample from the mobile domain, electrical resistivity tomography (ERT) is sensitive to bulk electrical conductivity and, thus, electrolytic solute in both the mobile and immobile domains. We demonstrate the new approach, in which temporal moments of co-located mobile-domain conductivity (i.e., conventional sampling) and ERT-estimated bulk conductivity are used to calculate heterogeneous mass-transfer rate and immobile porosity fractions in a series of numerical column experiments.

1. Introduction

Understanding the rates, scaling behavior, and heterogeneity of mass transfer is critical to the reliable prediction of contaminant transport and design of aquifer-remediation schemes. Complex concentration tailing and rebound in fractured and heterogeneous porous media have been explained by mass transfer [e.g., *Haggerty and Gorelick*, 1994; *Harvey et al.*, 1994a; *Haggerty and Gorelick*, 1995; *Benson et al.*, 2000; *Feehley et al.*, 2000; *Harvey and Gorelick*, 2000; *Dentz and Berkowitz*, 2003]. In models of mass transfer, an aquifer is conceptualized as consisting of multiple, overlapping continua. In the simplest formulation, a representative elementary volume is a bicontinuum consisting of (1) a mobile domain, in which advection and dispersion occur, and (2) an immobile domain, in which diffusion dominates. For the case without sorption,

$$\theta_m \frac{\partial c_m}{\partial t} + \theta_{im} \frac{\partial c_{im}}{\partial t} = \nabla \cdot \left(\theta_m D \nabla c_m\right) - \theta_m v \cdot \nabla c_m \text{, and} \tag{1a}$$

$$\frac{\partial c_{im}}{\partial t} = \alpha (c_m - c_{im}) , \tag{1b}$$

where c_m is the mobile-domain concentration [M/L^3], c_{im} is the immobile-domain concentration [M/L^3], D is the hydrodynamic dispersion tensor [L^2/T], v is the pore water velocity [L/T], θ_m is the mobile-domain porosity [-], θ_{im} is the immobile-domain porosity [-], α is the mass-transfer rate coefficient [T^{-1}], t is time [T]. Solute transfers between domains according to **(1b)**, residing in the immobile domain for an average period of $1/\alpha$; hence mass transfer produces breakthrough curves with long tails compared to standard advective-dispersive transport. Although linear exchange (**1b**) is commonly assumed, more complicated multi-rate models exist [*Haggerty and Gorelick*, 1995; *Berkowitz et al.*, 2006]. Mass transfer is thought to occur at the microscopic (e.g., grains), mesoscopic (e.g.,

fractures), and macroscopic (e.g., hydrofacies) scales [*Haggerty and Gorelick*, 1994; *Feehley et al.*, 2000; *Harvey and Gorelick*, 2000].

Experimental verification and measurement of the parameters controlling mass transfer (i.e., α and θ_{im}) is difficult because conventional sampling draws fluid from the mobile domain and provides only indirect information about the concentration in the immobile domain. Even with extensive coring, it is not possible to sample all scales of heterogeneity in a system, and insight into immobile solute and transfer rates remains problematic. For these reasons, the prevalence of mass transfer remains an issue of debate [*Hill et al.*, 2006; *Molz et al.*, 2006].

Recently, *Singha et al.* [2007] presented experimental data and numerical results indicating that mass transfer has an observable geoelectrical signature. Geoelectrical measurements are sensitive to total concentration of ionic species, rather than just mobile concentration. Experimental data collected during a push-pull freshwater injection into a brackish aquifer showed a hysteretic relation between co-located measurements of bulk and fluid conductivity; these findings are inconsistent with standard advective-dispersive behavior and petrophysical theory [*Archie*, 1942] but were explained by transport models that consider mass transfer. *Singha et al.* [2007] qualitatively reproduced their field-experimental data using first-order, linear mass transfer, and a modified version of Archie's Law in which both mobile and immobile porosity contribute to electrolytic conduction. Here, we capitalize on this finding and past work relating the temporal moments of mobile and immobile concentration [*Harvey and Gorelick*, 1995] to calculate mass-transfer parameters using geoelectrical measurements and conventional fluid sampling.

2. Approach

Conventional approaches to estimate mass-transfer parameters involve calibration of analytical or numerical models using observations of mobile-domain concentrations at the laboratory scale [e.g., *Hollenbeck et al.*, 1999] or field scale [e.g., *Harvey et al.*, 1994; *Feehley et al.*, 2000]. Access to either total or immobile concentration would provide additional information for calibration. *Harvey and Gorelick* [1995] developed algebraic relations between the temporal moments of mobile- and immobile-domain concentration breakthrough curves. For certain boundary conditions, differences between the temporal moments of c_m and c_{im} are functions solely of α, θ_m, and θ_{im}, and are independent of heterogeneity. In the following sections, we present the petrophysical basis for geoelectrical monitoring of mass transfer and inference of heterogeneous mass-transfer parameters.

2.1 Basis for the geoelectrical signature of mass transfer

Electrical resistivity tomography (ERT) increasingly is used to monitor hydrologic processes such as transport of conductive tracers in the laboratory [e.g., *Binley et al.*, 1996; *Slater et al.*, 2002] and field [e.g., *Kemna et al.*, 2002; *Singha and Gorelick*, 2005, 2006]. The basis for such work is the sensitivity of bulk conductivity to pore-fluid conductivity, as described by Archie's Law [*Archie*, 1942]:

$$\sigma_b = a\sigma_f \theta_t^q \tag{2}$$

where σ_b is bulk conductivity [S/m]; σ_f is fluid conductivity [S/m]; θ_t is total porosity [-], the sum of mobile and immobile porosity; q is cementation exponent [-]; and a is a fitting parameter, which is a function of tortuosity. **Eq. (2)** is widely used to relate pore-fluid and bulk conductivity in the absence of surface conduction. Although surface conductance is neglected here, it can be addressed with an additional term [e.g., *Worthington*, 1985]. For a bicontinuum, the measured fluid conductivity is that of the mobile-domain, and thus co-located measurements of bulk and fluid conductivity may depart from Archie's Law depending on mass-transfer. Assuming that electrolytic conduction occurs in both domains, we use a modified petrophysical model for the bicontinuum [after *Singha et al.*, 2007]:

$$\sigma_b = a\left(\theta_m + \theta_{im}\right)^{q-1}\left(\theta_m\sigma_{f,m} + \theta_{im}\sigma_{f,im}\right), \tag{3}$$

where $\sigma_{f,m}$ is the mobile conductivity [S/m]; $\sigma_{f,im}$ is the immobile conductivity [S/m]; θ_m is the mobile domain porosity [-]; θ_{im} is the immobile porosity [-]. We assume here that (1) the fitting parameter a is an effective value for the bicontinuum, and (2) bulk electrical conductivity varies linearly with total concentration [e.g., *Keller and Frischknecht*, 1966], and thus the conductivity of mobile and immobile porosities average arithmetically, i.e., as resistors in parallel. This petrophysical model could be adapted for situations where (1) either geometric or harmonic averaging is required, or (2) the tortuosities of mobile and immobile domains are known independently.

In ERT, an electrical gradient is established between two source electrodes, and voltages are measured between pairs of receiver electrodes. This procedure is repeated for many 4-electrode combinations. Typical ERT datasets comprise hundreds or thousands of measurements. Modern multi-channel instruments are capable of collecting multiple potential measurements simultaneously, allowing for rapid data acquisition (i.e., thousands of data per hour).

We simulate ERT data for column experiments using the EIDORS finite-element codes [*Adler and Lionheart*, 2006], which permit use of an irregular mesh of tetrahedral elements to accurately represent the column's cylindrical boundary. The ERT inverse problem involves minimization of an objective function combining two terms: (1) the least-squares, weighted misfit between observed and predicted measurements, and (2) a measure of solution complexity based on a 2nd-derivative spatial filter. The terms are weighted to achieve consistency between simulated and observed measurement errors, i.e., Occam's inversion [*Constable et al.*, 1987].

2.2 Inference of mass transfer parameters

Temporal moments are commonly used to describe breakthrough curves. The zero- through second-order moments are related to total mass, mean arrival time, and spread, respectively, and are commonly used to infer the rates of decay, advection and dispersion. Higher order moments are required to describe yet more complicated breakthrough (i.e., skewed or multi-peak). The n^{th} temporal moment, m_n, is defined as,

$$m_n = \int_0^\infty t^n c(t)\, dt\,. \tag{4}$$

where $c(t)$ is concentration at time t [e.g., *Goltz and Roberts*, 1987].

Harvey and Gorelick [1995] derived temporal moment-generating equations for linear and diffusive models of mass transfer under steady-state flow conditions. For certain boundary conditions, the temporal moments of c_m and c_{im} at a given location are related by simple algebraic expressions. For example, under linear mass transfer (**1b**):

$$m_n^{im} = n!\sum_{i=0}^{n} \frac{m_i^m}{i!}\frac{1}{\alpha^{n-i}} + n!\frac{c_{im}^0}{\alpha^n} \tag{5}$$

where, c_{im}^0 is the initial immobile concentration at the observation location; and m_n^m, m_n^{im} are the n^{th}-order temporal moments of mobile and immobile concentration, respectively. From **(5)**, it is evident that given temporal moments of co-located mobile and immobile concentration, it is possible to calculate mass-transfer rate coefficient and porosity fractions. For example, the mean arrival time of immobile concentration is offset from that of mobile concentration by a constant, which is a function of α, and this offset is independent of heterogeneity (in α or permeability).

Standard geochemical sampling cannot measure c_{im}, so we instead focus on total concentration (solute mass divided by bulk volume), which for electrolytes can be inferred using geoelectrical methods. Combining the definition of total concentration and **(5)**,

$$m_n^T = \frac{1}{\theta_m + \theta_{im}} \left(\theta_m m_n^m + \theta_{im} n! \sum_{i=0}^{n} \frac{m_i^m}{i!} \frac{1}{\alpha^{n-i}} + n! \frac{S_0}{\alpha^n} \right), \tag{6}$$

where m_n^T is the n^{th} temporal moment of total concentration. Consequently, given temporal moments of co-located mobile and total concentration, we can estimate α and porosity fractions for various initial conditions, S_0.

For purge experiments, in which immobile and mobile concentration are initially in equilibrium, consideration of temporal moments up to order one produces sufficient non-redundant equations to solve for mass-transfer parameters:

$$\alpha = \frac{m_0^T - m_0^m}{m_1^T - m_1^m - m_0^m \left(m_0^T - m_0^m \right) / S_0}, \tag{7}$$

$$\frac{\theta_{im}}{\theta_{im} + \theta_m} = \frac{\left(m_0^T - m_0^m \right)^2}{S_0 \left(m_1^T - m_1^m \right) - m_0^m \left(m_0^T - m_0^m \right)}, \text{ and} \tag{8}$$

$$\frac{\theta_m}{\theta_{im} + \theta_m} = 1 - \frac{\left(m_0^T - m_0^m \right)^2}{S_0 \left(m_1^T - m_1^m \right) - m_0^m \left(m_0^T - m_0^m \right)} \ . \tag{9}$$

For an invading solution with non-zero concentration, moments would be calculated based on differences between the injected and background concentrations. Pulse injections of tracer could also be considered; however, moments up to order two are required for the case of zero initial immobile concentration, and calculation of higher-order moments is more prone to error and the limits of ERT resolution than that of lower-order moments. Here, we focus on purge tests, although extension to pulse injections is trivial.

Eqns. (7-9) constitute a framework in which to calculate mass-transfer parameters from the temporal moments of mobile-domain concentration (i.e., from sampling) and total concentration or surrogate geoelectrical measurements. The procedure is straightforward and does not require inverse modeling. We note, however, that (1) these calculations are based on simple boundary conditions and assume steady-state flow; (2) reliable inference of temporal moments can prove difficult with sharp peaks and (or) strong tailing behavior with truncated breakthrough curves; and (3) the resolving power of geophysical tomography is limited by acquisition geometry, regularization, and measurement error [*Day-Lewis and Lane,* 2004*; Day-Lewis et al*., 2005, 2007].

3. Numerical Examples

We use numerical laboratory-scale column experiments to demonstrate geoelectrical inference of mass transfer parameters and to evaluate the limitations of the approach. Technology for ERT in columns is well established [e.g., *Binley et al.*, 1996]. As discussed in Section 2.2, we use the EIDORS toolbox [*Adler and Lionheart*, 2006] to simulate 3-D ERT data and our own ERT inverse code, which is based on Occam's inversion and smoothness-based regularization. MT3DMS [*Zheng and Wang*, 1999] is used to simulate solute transport with first-order mass transfer. We note that different conventions are used for the mass-transfer coefficient, α. As formulated in **(1)**, α is equivalent to the inverse of residence time in the immobile domain, whereas in MT3DMS, α is equivalent to immobile porosity divided by immobile residence time; hence values reported here were multiplied by θ_{im} for input to MT3DMS.

The experimental design for the column apparatus is summarized in Table 1. For simplicity, transport through the column is assumed to be one-dimensional, dispersion is neglected, flow is driven by an imposed head difference across the column, and hydraulic conductivity is homogeneous. The finite-difference grid for flow and transport consists of 1-cm cells. A constant-concentration boundary condition for the mobile domain is used at the input end of the column to simulate invasion into the mobile domain. The discharge boundary is modeled as an advective-flux condition. Prior to the purge experiment, the mobile and immobile domains are in equilibrium.

Table 1. Setup for synthetic column experiments.

Parameter	Value
Specific discharge	0.1 m/d
Head gradient	0.01
Hydraulic conductivity, K	10 m/d
S_0	1000 mg/l
Injection concentration	100 mg/l
θ_m, θ_{im}	0.1, 0.25
Cross sectional diameter	10 cm
Column length	100 cm
Archie a, q	1, 1
Rate constant, α, for homogeneous columns	0.95, 0.286, 0.095 s^{-1}
Rate constant, α, for heterogeneous column	0.8, 0.4, 0.28 s^{-1}

For the ERT apparatus, we assume a total of 24 electrodes arranged in two rows of 12, with rows parallel to the column axis and 180° apart (**fig. 1a,b**). Electrodes are modeled as 0.5-cm square pads consisting of multiple elements. The finite-element mesh comprises 18,420 tetrahedral elements. Current injections involve only 12 electrodes on one side of the column, in skip-1 configurations as described in *Slater et al.* [2000]. For a given current pair, voltages are measured for all remaining electrode pairs for which (1) geometric factors are less than 250, and (2) numerically calculated geometric factors differ by less than 1% between simulations using different homogeneous conductivity fields; these criteria eliminate data for which model noise is large relative to simulated voltages. The resulting acquisition geometry consists of 1573 measurements for each time-lapse dataset, which would take perhaps 30-60 min to collect given current technology. Simulated ERT datasets are collected at 3-hr intervals for 25 d. Gaussian errors with zero mean and 1.5% standard deviation are added to the simulated data and used also for weighting measurements in the inversion. The average pore-fluid velocity (10 m/day) is slow relative to data collection; hence temporal smearing should be negligible. Inversion parameters correspond to patches of elements in 5-cm intervals along the column.

We consider numerical examples for scenarios involving (1) homogeneous α, over a range from 0.1 to 1 d^{-1}; and (2) zonal heterogeneity of α. For the purpose of illustration, we assume fluid sampling can occur anywhere in the column, although in practice only a few ports or probes would be used or required. Temporal moments are calculated for time-series of ERT-estimated bulk conductivity and sampled fluid conductivity at 10-cm intervals along the column (e.g., **fig. 1c,d,e**), and α and θ_{im}/θ_t are calculated using (**7-8**), after differencing both series to account for the conductivity of the injectate and normalizing the ERT estimates by the ratio of the initial mobile to initial bulk conductivity. The results for homogeneous (**fig. 2a**) and heterogeneous columns (**fig. 2b**) indicate that our approach produces accurate estimates of mass-transfer parameters for about an order-of-magnitude range in α. For this example, α above approximately 1.0 d^{-1} results in exchange between domains so rapid that the breakthrough curves for c_m and c_{im} are near equilibrium and the calculated first moments are unreliable. Conversely, for α below approximately 0.1 d^{-1}, the exchange between domains is so slow that the immobile domain is not purged effectively during the 25-d experiment, resulting in truncated breakthrough curves and spurious estimates of temporal moments. Truncation results in overestimates of α (**fig. 2a**), with the bias worst toward the discharge end of the column, which is purged last and least effectively. These insights into experiment design and limitations can be explained and

predicted using the Damkohler number, *DaI*, a dimensionless measure of the effect of mass-transfer relative to advection [e.g., *Bahr and Rubin*, 1987]:

$$DaI = \frac{\alpha\left(1+\theta_{im}/\theta_{m}\right)L}{v} \quad . \tag{10}$$

where v is pore-fluid velocity and L is the domain length. For the assumed experimental setup, the approach is effective for $0.333 < DaI < 3.33$ (**fig. 2a**). We stress that the limitations discussed can be addressed by experiment design (i.e., column length, experiment duration, discharge rate) to achieve favorable *DaI* given the material under study; furthermore, these limitations are not specific to our framework but also impact conventional measurement of mass transfer [e.g., *Wagner and Harvey*, 1997; *Wörman and Wachniew*, 2007].

4. Discussion and Conclusions

New approaches are required for experimental verification and measurement of heterogeneous mass-transfer parameters. Recent work suggests that mass transfer manifests an observable geoelectrical signature, and that geoelectrical monitoring of tracer tests can provide insight into mass-transfer. We presented a framework in which to calculate heterogeneous mass-transfer rate coefficients and porosity fractions based on the temporal moments of co-located (1) fluid electrical conductivity, and (2) bulk electrical conductivity from ERT. Numerical experiments for laboratory-scale columns demonstrated the approach's potential, as well as its limitations. A given experimental design provides robust estimates over only a finite range of rate coefficient. We used the experimental Damkohler number, *DaI*, to bound the utility of our approach and provide guidelines for experiment design. We achieved good results for $0.333 < DaI < 3.33$. For experiments with greater *DaI*, the mobile and immobile domains are in approximate local equilibrium, with negligible separation between breakthrough curves. For lower *DaI*, the immobile domain is not purged during the experiment, leading to truncated breakthrough curves and biased estimate. The column length, discharge rate, and experiment duration must, therefore, be selected in combination and with consideration of the material under study; moreover, the ERT acquisition must be sufficiently rapid to resolve breakthrough.

Although this study focused on column-scale numerical experiments, our results have clear implications for improved characterization of parameters that control field-scale transport in aquifer and fluvial systems, where mass transfer limits the efficiency of aquifer storage and recovery [*Culkin et al.*, 2008] and remediation [*Haggerty and Gorelick*, 1994] activities. ERT can provide time-lapse information over a broad range of spatial scales, and our

approach could be adapted for analysis of field-scale tracer tests or extended through (1) inverse modeling to consider more complicated, multi-rate models of mass transfer, or (2) incorporation of approaches to improve moment inference and address truncated breakthrough curves [e.g., *Jose and Cirpka*, 2004; *Wörman and Wachniew*, 2007].

Acknowledgments

This work was funded by the U.S. Geological Survey Toxic Substances Hydrology and Ground-Water Resources Programs, and American Chemical Society PRF Grant 45206-G8 to KS. The authors are grateful to John W. Lane, Jr. and Rory Henderson (USGS) for comments on this work, and to Lee Slater, Olaf Cirpka, and an anonymous reviewer for useful suggestions and comments on the draft manuscript.

References

Adler, A. and W. R. B. Lionheart, Uses and abuses of EIDORS: An extensible software base for EIT, *Physiological Measurement,* 27: S25-S42, doi:10.1088/0967-3334/27/5/S03, 2006.

Archie, G. E., The electrical resistivity log as an aid in determining some reservoir characteristics, *Transactions of the American Institute of Mining, Metallurgical and Petroleum Engineers,* 146: 54-62, 1942.

Bahr, J. M., and J. Rubin, Direct comparison of kinetic and local equilibrium formulations for solute transport affected by surface reactions, *Water Resour. Res*., *23* (3), 438–452, 1987.

Benson, D. A., S. W. Wheatcraft and M. M. Meerschaert, Application of a fractional advection-dispersion equation, *Water Resour. Res.,* 36(6): 1403-1412, 2000.

Berkowitz, B., A. Cortis, M. Dentz and H. Scher, Modeling non-Fickian transport in geological formations as a continuous time random walk, *Reviews of Geophysics,* 44: RG2003, doi:10.1029/2005RG000178, 49 pp., 2006.

Binley, A., S. Henry-Poulter and B. Shaw, Examination of solute transport in an undisturbed soil column using electrical resistance tomography, *Water Resour. Res.,* 32(4): 763-769, 1996.

Jose, S.C. and O.A. Cirpka, Measurement of mixing-controlled reactive transport in homogeneous porous media and its prediction from conservative tracer test data, *Environ. Sci. Technol.*, 38 (7): 2089-2096, 2004.

Constable, S. C., R. L. Parker and C. G. Constable, Occam's inversion: a practical algorithm for generating smooth models from electromagnetic sounding data, *Geophysics,* 52: 289-300, 1987.

Culkin, S.L., Kamini Singha, and F.D. Day-Lewis, Implications of rate-limited mass transfer for aquifer storage and recovery, *Groundwater*, 2008, in press, doi: 10.1111/j.1745-6584.2008.00435.x, 16 p.

Day-Lewis, F. D., and J. W. Lane Jr., 2004, Assessing the resolution-dependent utility of tomograms for geostatistics, Geophysical Research Letters, 31, L07503, doi:10.1029/2004GL019617, 4p.

Day-Lewis, F. D., K. Singha, and A. M. Binley, 2005, Applying petrophysical models to radar traveltime and electrical resistivity tomograms: Resolution-dependent limitations, Journal of Geophysical Research, 110: B08206, doi:10.1029/2004JB005369, 17 p.

Day-Lewis, F.D., Y. Chen, and K. Singha, 2007, Moment Inference from Tomograms, *Geophysical Research Letters*, 34, L22404, doi: 10.1029/2007GL031621, 6p.

Dentz, M. and B. Berkowitz, Transport behavior of a passive solute in continuous time random walks and multirate mass transfer, *Water Resour. Res.,* 39(5): 10.1029/2001WR001163, 2003.

Feehley, C. E., C. Zheng and F. J. Molz, A dual-domain mass transfer approach for modeling solute transport in heterogeneous aquifers: Application to the Macrodispersion Experiment (MADE) site, *Water Resour. Res.,* 36(9): 2501-2516, 2000.

Goltz, M.N., and P.V. Roberts, Using the method of moments to analyze three-dimensional diffusion-limited solute transport from temporal and spatial perspectives, *Water Resources Research*, 23 (8), 1575-1585, 1987.

Haggerty, R. and S. M. Gorelick, Design of multiple contaminant remediation: Sensitivity to rate-limited mass transfer, *Water Resour. Res.,* 30(2): 435-446, 1994.

Haggerty, R. and S. M. Gorelick, Multiple-rate mass transfer for modeling diffusion and surface reactions in media with pore-scale heterogeneity, *Water Resour. Res.,* 31(10): 2383-2400, 1995.

Harvey, C. and S. M. Gorelick, Rate-limited mass transfer or macrodispersion: Which dominates plume evolution at the Macrodispersion Experiment (MADE) site?, *Water Resour. Res.,* 36(3): 637-650, 2000.

Harvey, C. F. and S. M. Gorelick, Temporal moment-generating equations: Modeling transport and mass transfer in heterogeneous aquifers, *Water Resour. Res.,* 31(8): 1895-1911, 1995.

Harvey, C. F., R. Haggerty and S. M. Gorelick, Aquifer remediation: A method for estimating mass transfer rate coefficients and an evaluation of pulsed pumping, *Water Resour. Res.,* 30(7): 1979-1992, 1994.

Hill, M. C., H. C. Barlebo and D. Rosbjerg, Reply to comment by F. Molz et al. on “Investigating the Macrodispersion Experiment (MADE) site in Columbus, Mississippi, using a three-dimensional inverse flow and transport model”, *Water Resour. Res.,* 42: W06604, doi:10.1029/2005WR004624, 2006.

Hollenbeck, K. J., C. F. Harvey, R. Haggerty and C. J. Werth, A method for estimating distributions of mass transfer rate coefficients with application to purging and batch experiments, *Journal of Contaminant Hydrology,* 37: 367-388, 1999.

Jose, S.C. and O.A. Cirpka, Measurement of mixing-controlled reactive transport in homogeneous porous media and its prediction from conservative tracer test data, *Environ. Sci. Technol.*, 38 (7): 2089-2096, 2004.

Keller, G. V. and F. C. Frischknecht, *Electrical Methods in Geophysical Prospecting*, Oxford, Pergamon Press, 523, 1966.

Kemna, A., J. Vanderborght, B. Kulessa and H. Vereecken, Imaging and characterisation of subsurface solute transport using electrical resistivity tomography (ERT) and equivalent transport models, *J. of Hydrology,* 267: 125-146, 2002.

Molz, F. J., C. Zheng, S. M. Gorelick and C. F. Harvey, Comment on "Investigating the Macrodispersion Experiment (MADE) site in Columbus, Mississippi, using a three-dimensional inverse flow and transport model" by Heidi Christiansen Barlebo, M.C. Hill, and D. Rosbjerg, *Water Resour. Res.,* 42: W06603, doi:10.1029/2005WR004265, 2006.

Singha, K. and S. M. Gorelick, Saline tracer visualized with electrical resistivity tomography: field scale moment analysis, *Water Resour. Res.,* 41: W05023, doi:10.1029/2004WR003460, 2005.

Singha, K. and S. M. Gorelick, Effects of spatially variable resolution on field-scale estimates of tracer concentration from electrical inversions using Archie's law, *Geophysics,* 71(3): G83-G91, 2006.

Singha, K., F. D. Day-Lewis and J. W. Lane, Jr., Geoelectrical evidence for bicontinuum transport in groundwater, *Geophys. Res. Letters,* 34: L12401, doi:10.1029/2007GL030019, 2007.

Slater, L., A. M. Binley, W. Daily and R. Johnson, Cross-hole electrical imaging of a controlled saline tracer injection, *J. of Applied Geophysics,* 44(2-3): 85-102, 2000.

Slater, L., A. Binley, R. Versteeg, G. Cassiani, R. Birken and S. Sandberg, A 3D ERT study of solute transport in a large experimental tank, *J. App. Geophys.,* 49: 211-229, 2002.

Wagner, B.J., and J.D. Harvey, Experimental design for estimating parameters of rate-limited mass transfer: Analysis of stream tracer studies, *Water Resour. Res.*, 33 (7), 1731–1741, 1997.

Wörman, A., and P. Wachniew, Reach scale and evaluation methods as limitations for transient storage properties in streams and rivers, *Water Resour. Res.*, 43, W10405, doi:10.1029/2006WR005808, 2007.

Worthington, P.F., Evolution of shaley sand concepts in reservoir evaluation, *The Log Analyst*, 26, 23-40, 1985.

Zheng, C. and P. P. Wang, *MT3DMS: A modular three-dimensional multispecies model for simulation of advection, dispersion and chemical reactions of contaminants in groundwater systems: documentation and user's guide*, Report SERDP-99-1. Vicksburg, Mississippi, U.S. Army Engineer Research and Development Center, 202, 1999.

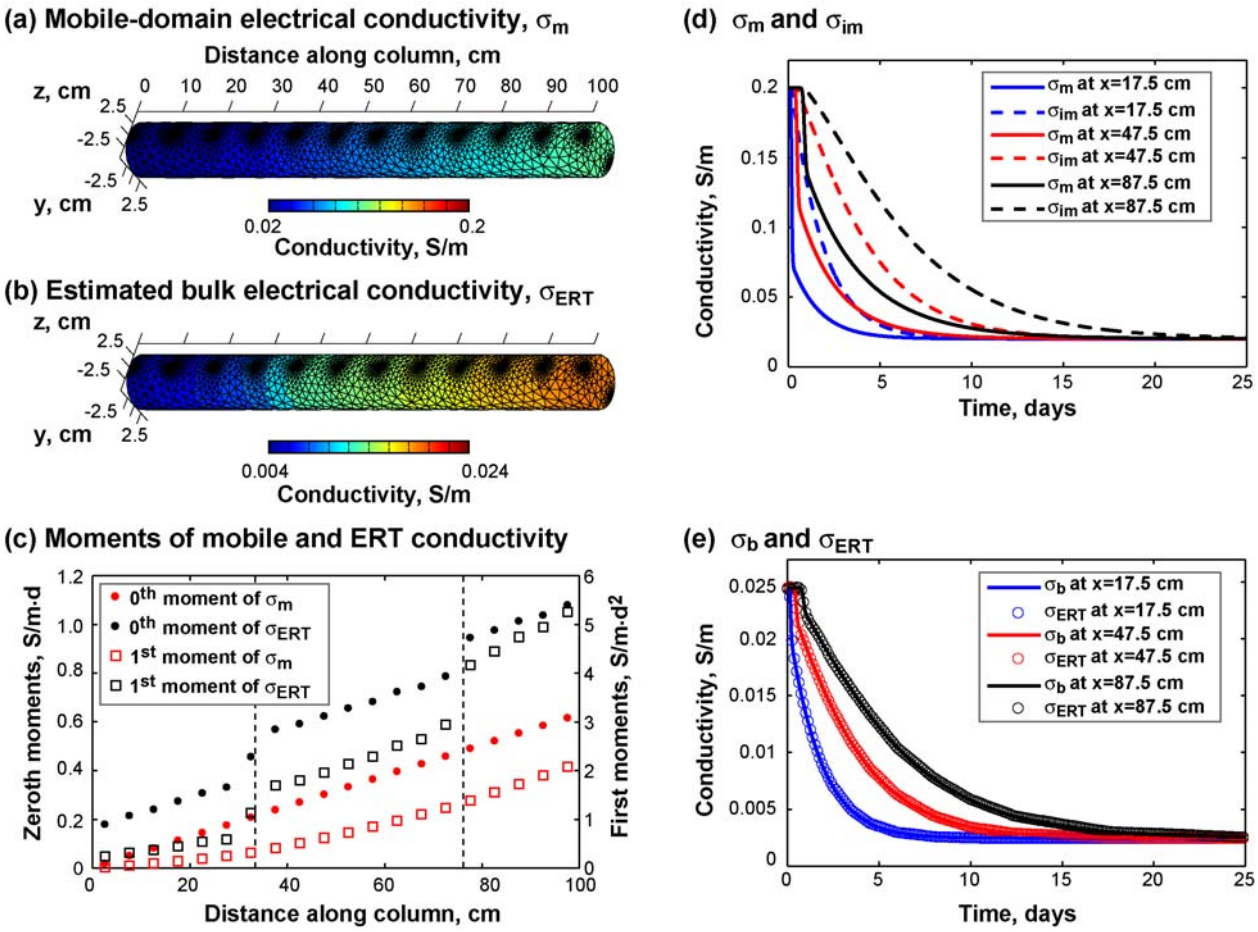

Figure 1. For the heterogeneous column (a) Mobile-domain fluid conductivity within the finite-element mesh at 2.5 days after start of injection; (b) estimated bulk electrical conductivity from electrical resistivity tomography (ERT) at 2.5 days; (c) temporal moments of mobile-domain fluid conductivity and estimated bulk electrical conductivity; (d) breakthrough curves of mobile-domain and immobile-domain fluid conductivity at three locations; and (e) estimated and true bulk conductivity at three locations. Dashed lines in (c) indicate zonation for heterogeneous rate constant.

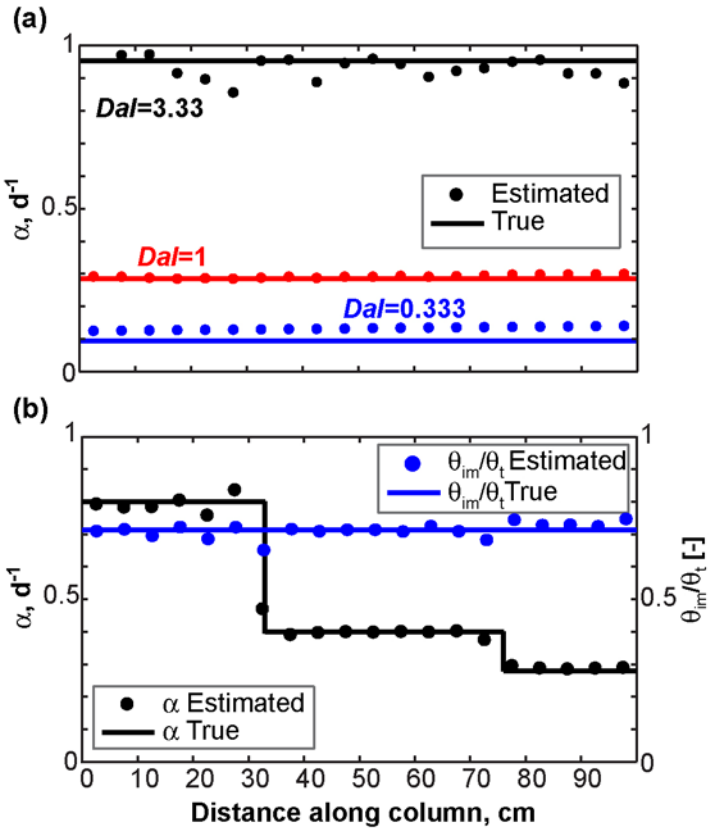

Figure 2. (a) Estimated and true rate coefficient, α, for three homogeneous columns with Damkohler numbers, DaI, of 0.333, 1 and 3.33; (b) estimated and true rate coefficient and immobile-porosity fraction for the heterogeneous column.